

# Hydrocarbon Chain Lengthening in Catalytic CO Hydrogenation: Evidence for a CO-Insertion Mechanism

Julien Schweicher,<sup>†</sup> Adam Bundhoo, and Norbert Kruse\*

Chemical Physics of Materials (Catalysis-Tribology), Université libre de Bruxelles, Campus Plaine, CP 243, 1050 Brussels, Belgium

**S** Supporting Information

**ABSTRACT:** We studied CO hydrogenation over Co/MgO (10/1) model catalysts using chemical transient kinetics. Quantification of the time-dependent response during fast changes of the gas flow composition enabled the counting of surface amounts of carbon, oxygen, and hydrogen from the onset of adsorption to the steady state of the reaction and vice versa. Under the atmospheric pressure conditions of the reaction, the total amount of adsorbed species exceeded the monolayer limit on Co metal. The time response in transients and back-transients of gaseous reactants and products is in accordance with a CO insertion mechanism. Furthermore, the Anderson–Schulz–Flory chain lengthening probability is directly proportional to the CO pressure, whereas no such dependence is measured for the amounts of accumulating or fading surface carbon.

The question of the microscopic mechanism of chain lengthening in the catalytic production of hydrocarbons from carbon monoxide and hydrogen is as old as the reaction itself. Fischer and Tropsch, after first reporting on “synthol” formation (a mixture of oxygenates as part of an “oily fraction”) in the high-pressure process,<sup>1</sup> considered several options until they finally advocated a carbide-type mechanism on account of atmospheric pressure data.<sup>2</sup> Within this mechanism, carbides were assumed to react with hydrogen so as to provide surface methylene which acts as a building group (or “monomer”) for hydrocarbon formation via polymerization. These original ideas, supported by additional experimental evidence in the early 1980s,<sup>3–6</sup> have largely been retained up to the present, where research aims at qualifying the very nature of the CH<sub>x</sub> species involved in C–C coupling<sup>7–12</sup> or insertion into a metal–alkyl bond.<sup>13</sup>

Several shortcomings of the original carbide-type mechanism, in particular the difficulties in explaining both hydrocarbon and oxygenate production, prompted several researchers to look for alternatives. Historically, after the original considerations by Fischer,<sup>14</sup> work with <sup>14</sup>C-carbided iron catalysts in the group of Emmett<sup>15</sup> led to the alternative view that a C<sub>x</sub>H<sub>y</sub>O<sub>z</sub> intermediate might actually be formed from molecular hydrogen and CO without dissociation of the latter.<sup>16,17</sup> The stoichiometry of this intermediate has remained a matter of debate up to the present.<sup>18</sup> In any case, however, the C–O bond has to be broken sooner or later so as to give way to the formation of hydrocarbons. Considering “late” C–O bond breaking, several mechanistic scenarios may be envisaged to

produce the relevant monomers needed for chain lengthening. For example, recent theoretical/experimental work has provided evidence for the formation of a formyl- and hydroxymethylene-type species as precursor of CH<sub>x</sub> monomer formation.<sup>19</sup> Similar suggestions were also previously made by others on the basis of energetic considerations using density functional theory (DFT).<sup>20,21</sup> Realizing that the hypothesis of a high surface coverage of monomeric CH<sub>x</sub> so as to ensure fast chain growth relative to chain termination would possibly not apply to real Fischer–Tropsch (FT) reaction conditions, Zhuo et al. adopted the alternative view of a CO insertion mechanism into a metal–carbon bond of surface RCH, thus forming RCHCO.<sup>22</sup> Again, this implies a “late” C–O bond scission, liberating R'CH<sub>3</sub> hydrocarbons (after further hydrogenation of RCHO surface aldehydes) while keeping CO in the adsorbed state. More generally, CO insertion (i.e., alkyl shift) is a viable mechanistic step in the homogeneous hydroformylation of alkenes. This was first shown by Heck and Breslow more than 50 years ago.<sup>23</sup> Nearly 10 years later, Pichler and Schulz<sup>24</sup> adopted the new (at that time) achievements of coordination chemistry to postulate adsorbed metal hydro-subcarbonyls (in particular, HRu(CO)<sub>x</sub>) to act as a pool for CO being inserted into a metal–alkyl bond.

Whatever the suggested mechanism, a general feature of many models seems to be a largely metallic surface during reaction. The present paper aims to demonstrate the importance of quantification and to consider “crowded” rather than “empty” surfaces under atmospheric pressure conditions of the FT reaction. Furthermore, experimental evidence will be provided in favor of a CO insertion mechanism to be responsible for chain lengthening and hydrocarbon production. The experimental evidence for drawing such far-reaching conclusions is based on studies using chemical transient kinetics (CTK) which is a relaxation-type technique originally developed by Wagner<sup>25</sup> and applied to heterogeneous catalysis by Tamaru<sup>26</sup> nearly 50 years ago.

Studies by CTK consist of subjecting the catalyst to sudden changes in the gas-phase chemical composition under controlled flow conditions. For the CO hydrogenation over Co/MgO studied here, first a flow of H<sub>2</sub> (using He as inert reference) was initiated so as to establish a dynamic adsorption/desorption equilibrium of H<sub>2</sub> at 230 °C. Next, the H<sub>2</sub>+He gas mixture was abruptly replaced by a reactive H<sub>2</sub>+CO/Ar flow while keeping constant the H<sub>2</sub> inlet flow as well as the total flow rate (Figure 1). This switch from H<sub>2</sub>+He

Received: July 20, 2012

Published: September 19, 2012

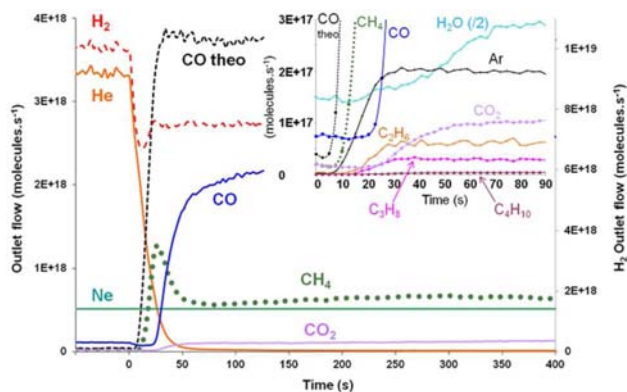


**Figure 1.** Outlet flows (molecules  $s^{-1}$ ) during the build-up experiment ( $T = 230\text{ }^{\circ}\text{C}$ ,  $p_{\text{tot}} = p_{\text{atm}}$ , total volumetric flow rate  $D_{\text{tot}} = 40\text{ cm}^3\text{ min}^{-1}$ , and  $\text{H}_2/\text{CO} = 3$ ). The time marker for the build-up stage is set to zero for the point in time at which Ar, i.e.,  $\text{CO}_{\text{theo}}$ , is first detected by the MS. The inset provides a zoom into the early stages of the build-up and allows identification of delay times.

to  $\text{H}_2/\text{CO}/\text{Ar}$  defined the beginning of the *build-up* of the reaction and led to the construction of the catalytically active surface. The addition of a small quantity (5%) of argon provided an inert reference for the characterization of the reactor gas-phase response in the presence of a catalyst bed and allowed the calculation of a theoretical CO response for the hypothetical case of no CO chemisorption occurring ( $\text{CO}_{\text{theo}}$  in Figure 1). Switching back from steady-state  $\text{H}_2/\text{CO}/\text{Ar}$  to initial nonreactive  $\text{H}_2/\text{He}$  initiated the *back-transient* and re-established the initial dynamic adsorption/desorption equilibrium of  $\text{H}_2$ .

Turning to the build-up first, Figure 1 reveals major delay times in the response to switching gases. All products lag behind the Ar reference (rescaled to provide  $\text{CO}_{\text{theo}}$ ). Moreover, a significant delay time is seen for the measured CO response. The inset in Figure 1 provides a zoom into the early build-up and reveals this time delay to be  $\sim 18\text{ s}$ ; i.e., during approximately 18 s, with reference to the  $\text{CO}_{\text{theo}}$  onset, the entire amount of CO entering the reactor is adsorbed on the catalyst surface. We also see that  $\text{CH}_4$  lags  $\sim 5\text{ s}$  behind  $\text{CO}_{\text{theo}}$ . Methane production subsequently runs through a maximum, and CO appears at that very moment. Moreover, chain lengthening essentially does not start before both the occurrence of CO and the maximum in  $\text{CH}_4$  production. This observation provides a first indication for CO acting as the  $\text{C}_1$  monomer in  $\text{C}_{2+}$  formation. Furthermore, and in line with this conclusion, the  $\text{C}_{2+}$  hydrocarbons appear in sequence; i.e.,  $\text{C}_2\text{H}_6$  is formed first, followed shortly by  $\text{C}_3\text{H}_8$  and  $\text{C}_4\text{H}_{10}$ . Finally, we note that the start of  $\text{CO}_2$  and  $\text{H}_2\text{O}$  production is time-correlated with the CO appearance, i.e.,  $\sim 18\text{ s}$  after the  $\text{CO}_{\text{theo}}$  signal. A CO steady-state conversion of 29% (the difference between measured CO and  $\text{CO}_{\text{theo}}$  after  $\sim 500\text{ s}$ ) is measured, corresponding to a reaction rate of  $0.94\text{ molecule s}^{-1}\text{ nm}^{-2}$  of Co surface area (see SI) or a turnover frequency of  $0.064\text{ molecule s}^{-1}\text{ site}^{-1}$ .

We mention here that the reported transient kinetic features were the same in measurements with 10% CO conversion. It is also interesting to note that similar build-up features were observed in CTK studies with other types of catalysts, such as mixed  $\text{CoCuMg}^{27}$  and Ni.<sup>28</sup>

The back-transient results are plotted in Figure 2 as relative outlet flows (by normalizing the absolute outlet flows to their

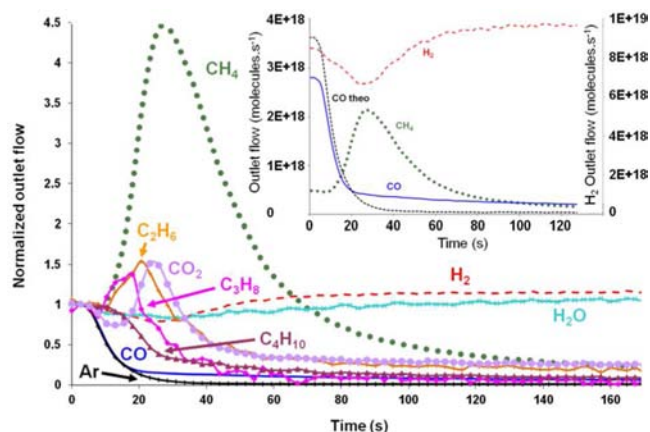


**Figure 2.** Normalized outlet flows during back-transient (same reaction conditions as in Figure 1). Inset: absolute outlet flows (molecules  $s^{-1}$ ).

steady-state values). As can be seen, switching from reactive  $\text{H}_2/\text{CO}/\text{Ar}$  to “scavenging”  $\text{H}_2/\text{He}$  conditions causes the CO outlet flow to drop exponentially with time. The CO and Ar curves actually appear superimposed, meaning that the time constants of removal from the reactor are very similar for both of them. Figure 2 also shows that, once the CO inlet flow stops, the  $\text{C}_{2+}$  hydrocarbon (and  $\text{CO}_2$ ) production decreases very quickly (after passing a short-term maximum of  $\sim 1.5$  times their steady-state values; see discussion below). Both the fast Ar-akin removal of CO and the cessation of hydrocarbon chain lengthening provide a second strong indication for weakly adsorbing CO playing the role of the  $\text{C}_1$  monomer.

The time-resolved hydrocarbon scavenging in back-transients calls for a more rigorous inspection. The fact that all hydrocarbons exhibit a maximum in Figure 2 before decreasing suggests surface emptying to be a two-step process. The maximum is, however, most pronounced for methane, meaning that its surface precursor is the most abundant surface intermediate (“*masi*”) among the precursors leading to hydrocarbon formation. In fact, the  $\text{CH}_4$  outlet flow reaches a maximum of 4.5 times its steady-state value before decreasing. This allows the simultaneous  $\text{H}_2$  consumption to be attributed mainly to  $\text{CH}_4$  formation (approximately two  $\text{H}_2$  molecules per  $\text{CH}_4$  molecule). Moreover, the *masi* can only contain one C atom (and, most probably, oxygen as well; see below). To explain the occurrence of a two-step process in hydrocarbon formation during back-transients, it may be safely assumed that the number of metallic surface sites first increases, thereby raising the atomic hydrogen supply after  $\text{H}_2$  dissociation. In the second step, the reactive transient species react with hydrogen to produce gaseous hydrocarbons with a common time constant of  $\sim 26\text{ s}$  in a pseudo-first-order kinetic process. To see this, the outlet flows are replotted on a logarithmic scale in Figure 3. To provide a guide to the eye, we have underlined the identical linear decay (time constant of  $\sim 26\text{ s}$ ) for methane and ethane removal (the decay times for  $\text{C}_3\text{H}_8$  and  $\text{C}_4\text{H}_{10}$ , while being similar to those of methane and ethane, are subject to a relatively large error of  $\sim 25\%$ ). As to Ar and CO, we find much shorter times,  $\tau_{\text{Ar}} = 8.2\text{ s}$  and  $\tau_{\text{CO}} = 7.8\text{ s}$ .

Taking  $\tau_{\text{Ar}} = 8.2\text{ s}$ , the reactor volume is obtained:  $5.5\text{ cm}^3$  (total volumetric flow rate:  $40\text{ cm}^3\text{ min}^{-1} = 0.67\text{ cm}^3\text{ s}^{-1}$ ). On the contrary, the time constants for hydrocarbons ( $\sim 26\text{ s}$ ) and  $\text{CO}_2$  (14.8 s) correspond to the combination of desorption from the catalyst surface and removal from the reactor by gas-

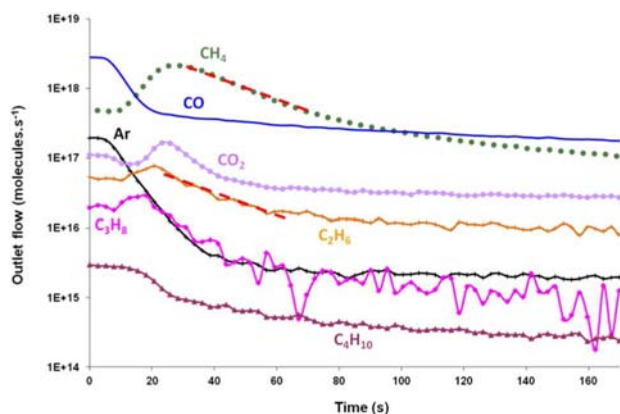


**Figure 3.** Outlet flows (molecules  $s^{-1}$ ) during back-transient (logarithmic scale). The extended tailing observed at long times is due to limitations resulting from the pumping speed.

phase transport. Their values are consequently larger than those of Ar and CO.

The propensity of a FT catalyst to produce long-chain hydrocarbons is usually expressed in terms of the Anderson–Schulz–Flory (ASF)<sup>29</sup> chain lengthening probability  $\alpha$ . In our case, for the atmospheric FT reaction on a Co/MgO model catalyst,  $\alpha = 0.2$  at steady state of the reaction. This relatively low value corresponds to a product spectrum of light hydrocarbons, in accordance with observations originally made by Fischer and Tropsch in 1926<sup>2</sup> and frequently reproduced thereafter.

The quantification of the CTK data in terms of atomic surface concentrations (“surface atom counting”; see SI) provides further clues for assessing the chain lengthening mechanism. Such counting is most straightforward for carbon and oxygen atoms, as the catalyst is essentially free of these species at the very instant of switching from hydrogen adsorption to CO+H<sub>2</sub> reaction conditions (see Figure 1). Therefore, surface carbon atom counting during the early build-up phase (from  $t = 0$  to 90 s) was used to establish Figure 4, in

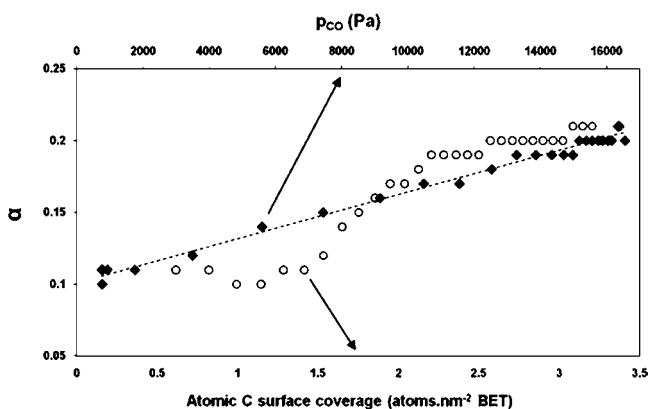


**Figure 4.** Evolution of  $\alpha$  as a function of  $p_{CO}$  and surface atomic C amounts during early stages of build-up.

which the ASF chain lengthening probability is plotted as a function of both the accumulating surface carbon and the CO gas-phase pressure. It is clearly seen that  $\alpha$  is proportional to  $p_{CO}$  (linear relationship), while no such dependence exists with respect to the surface carbon amounts. Even if the surface carbon species is associated with hydrogen atoms so as to form

adsorbed CH<sub>x</sub>, no linear dependence would result. This places a third strong argument in favor of a CO insertion mechanism to be in operation. On the basis of the obtained data, neither C–C coupling nor CH<sub>2</sub> insertion actually appears likely mechanisms for chain lengthening.

The experimental evidence of CO being the monomer responsible for chain lengthening in FT at atmospheric pressure raises questions about the nature and the formation mechanism of the *masi*. Notwithstanding the instantaneous detection of this *masi* being difficult, if not impossible, at this point in time, CTK may provide clues and either support or discard the various reaction models proposed in the literature. For reasons mentioned above, we limit the discussion to models that advocate a CO insertion mechanism. To do so, it is most instructive to consider the surface coverage under operating conditions. Respective data are obtained by evaluating the mass balance and integrating the atomic surface flows for C, O, and H atoms (see SI). Accordingly, the steady-state surface coverage is characterized by  $\sim 7$  C,  $\sim 10$  O, and  $\sim 7.5$  H atoms  $nm^{-2}$  of BET surface area (Co+MgO, with Co/Mg = 10; the hydrogen coverage does not take into account the initial value,  $\sim 15$  atoms  $nm^{-2}$ , corresponding to the dynamic adsorption–desorption equilibrium). These values suggest that the monolayer capacity is exceeded (the “oversaturation” is even more evident when scaling to Co only). Clearly, different molecular species contributing to the counted atoms may be present on the surface: CO, OH, H<sub>2</sub>O, CH<sub>x</sub>, formates, etc. Subsurface Co states may also be occupied. The important conclusion from these quantitative considerations is that the catalytically active Co surface does not present metallic properties under atmospheric CO+H<sub>2</sub> operating conditions. The surface is rather “crowded” instead. While the coverage information is rarely taken into account in mechanistic considerations, it imposes boundary conditions for model testing. More specifically, insertion of CO into a metal–adsorbate bond (Me–H or metal–alkyl) is rather unlikely for steric reasons. We recall that the experimental evidence from our back-transients is compatible with insertion of weakly adsorbed rather than chemisorbed CO. Adsorbed hydro-subcarbonyls, HMe(CO)<sub>x</sub>, suggested by Pichler and Schulz<sup>24</sup> to play the role of a precursor pool for CO insertion, have to be discarded for the same reason.

To further develop the CO insertion mechanism, it is instructive to discuss the time-dependent build-up features of Figure 1 in the light of the hydrogen-assisted CO activation reported by Ojeda et al.<sup>19</sup> Quite generally, the increasing hydrogen chemisorption after switching from H<sub>2</sub> adsorption to CO+H<sub>2</sub> reaction conditions is in agreement with this scenario so far as surface OH and CH groups are produced by dissociation of a primary oxygen-containing complex. Our time-dependent build-up studies demonstrate that no O-containing species (i.e., water and carbon dioxide) are detected within 18 s of switching the gas composition. Clearly, the catalytically active phase is under construction during this time period, and it is most likely that OH groups form then. In our opinion, the O–H bond in surface hydroxyl could then be the target for CO insertion. CH groups, on the other hand, undergo further hydrogenation and may leave the catalyst as methane  $\sim 5$  s after initiating the build-up (without water production). Thus, a sequence of CH<sub>x</sub> hydrogenation steps may explain the initially high methane production; however, it does not when running into the steady state of the reaction. The coincidence of the early maximum in methane production and the CO appearance

in the gas phase along with chain lengthening pleads for a different scenario which, according to our view, could involve the sustained formation of a formate-derived (or carboxylate-akin, under chain lengthening conditions) complex<sup>30</sup> that undergoes further hydrogenation to alkoxy surface groups and, finally, hydrocarbons (along with water and carbon dioxide). We note that such a mechanism would enable the production of paraffins as well as olefins and oxygenates within a “late” kinetic branching.

In summary, we have provided several experimental clues in favor of CO insertion to be responsible for chain lengthening in CO hydrogenation to hydrocarbons: (1) Chain lengthening occurs only when CO is present in the gas phase. (2) Since C<sub>2+</sub> gaseous products appear in the sequence of their carbon number, the chain lengthening process must involve a C<sub>1</sub> monomer, which is the case for CO. (3) Chain lengthening stops abruptly when CO is removed from the inlet flow during back-transients. (4) The chain lengthening factor  $\alpha$  exhibits a linear relationship with  $p_{\text{CO}}$  during the early stage of the build-up, while this is not the case for the atomic C (or CH<sub>x</sub>) surface coverage. The overall surface coverage of the investigated Co/MgO catalyst is larger than the monolayer capacity. Time-dependent build-up studies are in agreement with the scenario of hydrogen-assisted CO activation forming O–H groups,<sup>19</sup> which could be considered as the target for CO insertion.

## ■ ASSOCIATED CONTENT

### 📄 Supporting Information

Catalyst preparation and activation, CTK quantification, and surface atom counting. This material is available free of charge via the Internet at <http://pubs.acs.org>.

## ■ AUTHOR INFORMATION

### Corresponding Author

nkruse@ulb.ac.be

### Present Address

†Therapeutic Micro and Nanotechnology Laboratory, University of California, San Francisco

### Notes

The authors declare no competing financial interest.

## ■ ACKNOWLEDGMENTS

This paper is dedicated to the memory of Alfred Frennet. This work was financially supported by FRIFA (Ph.D. grants for J.S. and A.B.), which is gratefully acknowledged. We are also thankful for support by Shell Global Solutions.

## ■ REFERENCES

- (1) Fischer, F.; Tropsch, H. *Brennst. Chem.* **1923**, *4*, 276–285.
- (2) Fischer, F.; Tropsch, H. *Brennst. Chem.* **1926**, *7*, 97–104.
- (3) Brady, R. C.; Pettit, R. J. *Am. Chem. Soc.* **1980**, *102*, 6181–6182.
- (4) Brady, R. C.; Pettit, R. J. *Am. Chem. Soc.* **1981**, *103*, 1287–1289.
- (5) Bell, A. T. *Catal. Rev.-Sci. Eng.* **1981**, *23*, 203–232.
- (6) Chuang, S. C.; Tian, Y. H.; Goodwin, J. G.; Wender, I. J. *Catal.* **1985**, *96*, 396–407.
- (7) Ciobica, I. M.; Frechard, F.; van Santen, R. A.; Kleyn, A. W.; Hafner, J. *Chem. Phys. Lett.* **1999**, *311*, 185–192.
- (8) Ciobica, I. M.; Kramer, G. J.; Ge, Q.; Neurock, M.; van Santen, R. A. *J. Catal.* **2002**, *212*, 136–144.
- (9) Liu, Z.-P.; Hu, P. *J. Am. Chem. Soc.* **2002**, *124*, 11568–11569.
- (10) Gong, X.-Q.; Raval, R.; Hu, P. *J. Chem. Phys.* **2005**, *122*, 024711–6.

- (11) Cheng, J.; Gong, X.-Q.; Hu, P.; Lok, C. M.; Ellis, P.; French, S. J. *Catal.* **2008**, *254*, 285–295.
- (12) Cheng, J.; Hu, P.; Ellis, P.; French, S.; Kelly, G.; Lok, C. M. *J. Catal.* **2008**, *257*, 221–228.
- (13) Biloen, P.; Sachtler, W. M. H. *Adv. Catal.* **1981**, *30*, 165–216.
- (14) Fischer, F. *The Conversion of Coal into Oils*; Ernest Benn Ltd.: London, 1925.
- (15) Podgurski, H. H.; Kummer, J. T.; DeWitt, T. W.; Emmett, P. H. *J. Am. Chem. Soc.* **1950**, *72*, 5382–5388.
- (16) Storch, H. H.; Golumbic, N.; Anderson, R. B. *The Fischer–Tropsch and Related Syntheses*; Wiley: New York, 1951.
- (17) Vannice, M. A. *J. Catal.* **1975**, *37*, 462–473.
- (18) Davis, B. H. *Catal. Today* **2009**, *141*, 25–33.
- (19) Ojeda, M.; Nabar, R.; Nilekar, A. U.; Ishikawa, A.; Mavrikakis, M.; Iglesia, E. *J. Catal.* **2010**, *272*, 287–297.
- (20) Huo, C.-F.; Li, Y.-W.; Wang, J.; Jiao, H. *J. Phys. Chem. C* **2008**, *112*, 14108–14116.
- (21) Inderwildi, O. R.; Jenkins, S. J.; King, D. A. *J. Phys. Chem. C* **2008**, *112*, 1305–1307.
- (22) Zhuo, M.; Tan, K. F.; Borgna, A.; Saeys, M. *J. Phys. Chem. C* **2009**, *113*, 8357–8365.
- (23) Heck, R. F.; Breslow, D. S. *J. Am. Chem. Soc.* **1961**, *83*, 4023–4027.
- (24) Pichler, H.; Schulz, H. *Chem. Ing. Techn.* **1970**, *42*, 1162–1174.
- (25) Wagner, C.; Hauffe, K. *Z. Elektrochem.* **1939**, *45*, 409–425.
- (26) Tamaru, K. *Adv. Catal.* **1965**, *15*, 65–90.
- (27) Frennet, A.; Visart de Bocarmé, T.; Bastin, J.-M.; Kruse, N. *J. Phys. Chem. B* **2005**, *109*, 2350–2359.
- (28) Bundhoo, A.; Schweicher, J.; Frennet, A.; Kruse, N. *J. Phys. Chem. C* **2009**, *113*, 10731–10739.
- (29) Anderson, R. B.; Friedel, R. A.; Storch, H. H. *J. Chem. Phys.* **1951**, *19*, 313–319.
- (30) Schweicher, J.; Bundhoo, A.; Frennet, A.; Kruse, N.; Daly, H.; Meunier, F. C. *J. Phys. Chem. C* **2010**, *114*, 2248–2255.